Electronic Supplementary Information

Three-dimensional chiral networks of triboelectric nanogenerators as inspired by metamaterial's structure

Xianye Li,[ab] Liang Xu,*[ab] Pei Lin,*[ad] Xiaodan Yang,[ab] Huamei Wang,[ab] Huaifang Qin[ab] and Zhong Lin Wang*[ac]

[a] Beijing Institute of Nanoenergy and Nanosystems, Chinese Academy of Sciences, Beijing, 101400, P. R. China. E-mail: xuliang@binn.cas.cn

[b] School of Nanoscience and Technology, University of Chinese Academy of Sciences, Beijing, 100049, P. R. China.

[c] Georgia Institute of Technology, Atlanta, Georgia, 30332-0245, USA. E-mail: zlwang@gatech.edu

[d] Key Laboratory of Materials Physics of Ministry of Education, School of Physics and Microelectronics, Zhengzhou University, Zhengzhou, 450001, P. R. China. E-mail: linpei@zzu.edu.cn

Content

Supplementary Figures:

Supplementary Movies:

Movie S4 348 LEDs are lighted up by the parallel TENG network.

Movie S5 348 LEDs are lighted up by the serial TENG network.

Movie S6 Self-powered temperature and humidity sensing based on the 3D chiral TENG network.

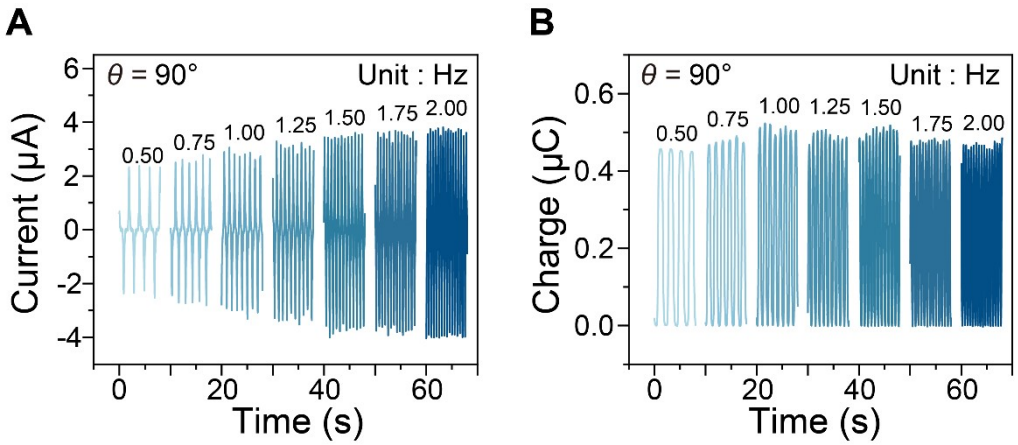

Fig. S1. Electrical characterization of the network unit. Dependence of short-circuit current (A) and transferred charges (B) on the rocking frequency for a single TENG.

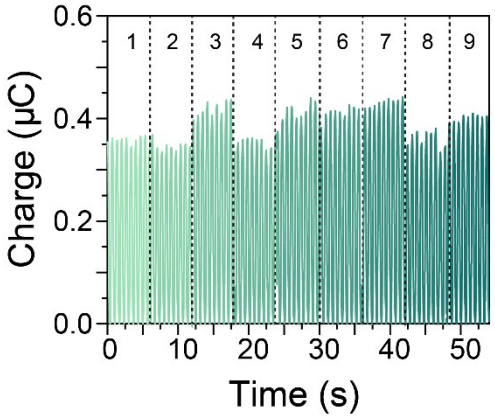

Fig. S2. Transferred charges of each TENG unit (numbered from 1 to 9) under harmonic agitations with $\theta = 90°$ and $f = 1.5$ Hz in air.

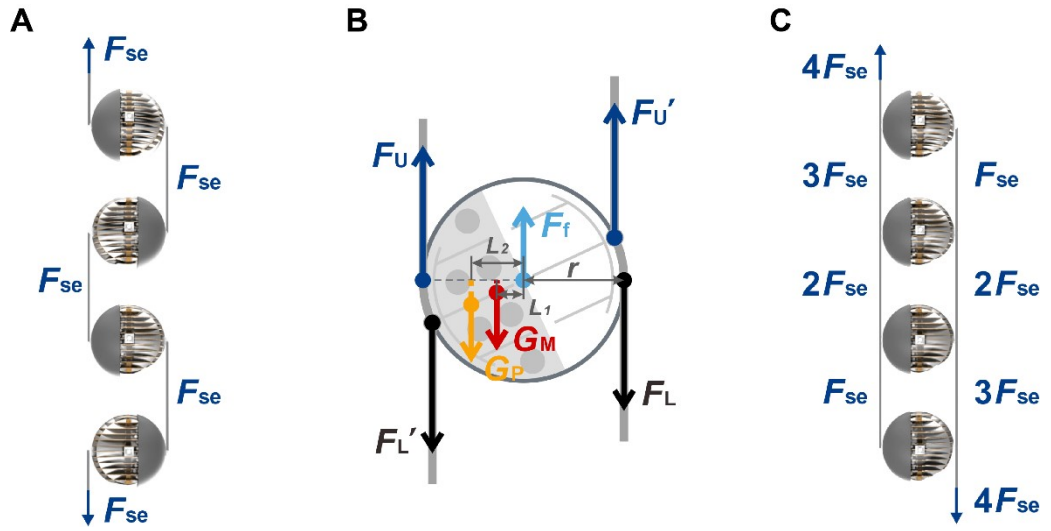

Fig. S3. Force analysis of chiral chains. (A) Ligament force in the serial chain. (B) Force analysis along the vertical direction of the chiral unit in the parallel chain. (C) Ligament force in the parallel chain.

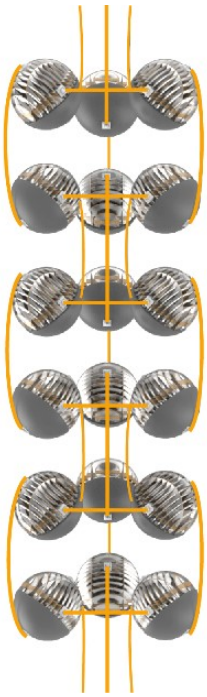

Fig. S4. Schematic illustration of the 3D chiral TENG network.

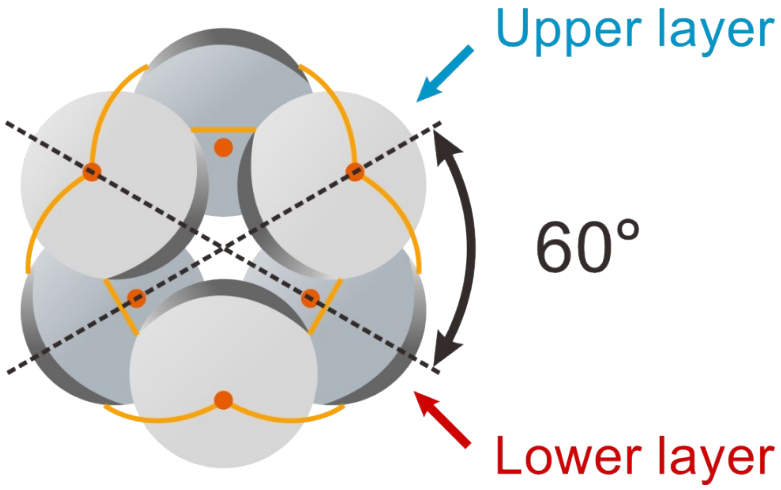

Fig. S5. Schematic illustration of interlayer shifting from the top view.

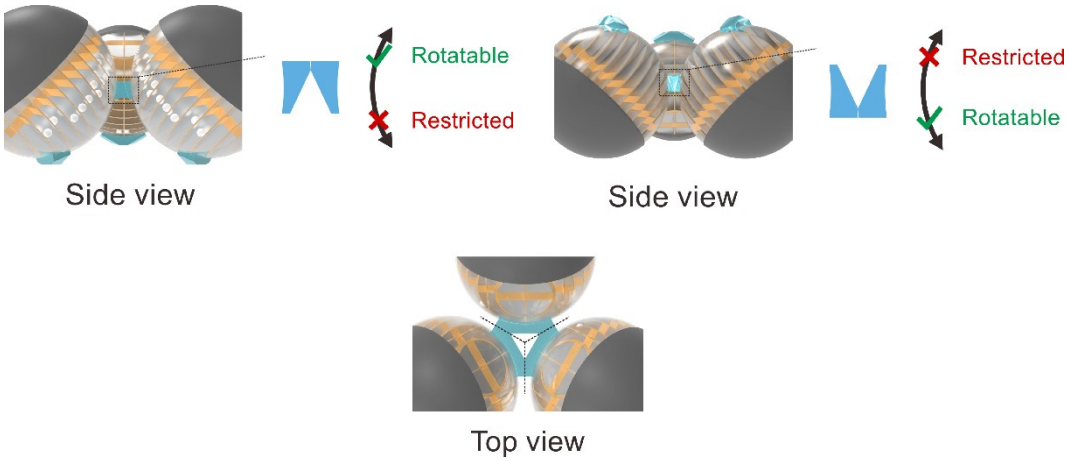

Fig. S6. Schematic illustrations of the limit block.

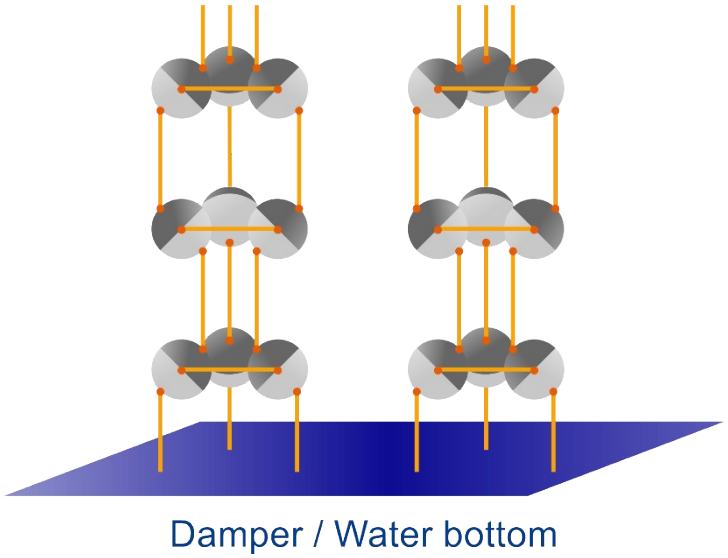

Fig. S7. Schematic illustration of the 3D chiral TENG network with the lower end constrained. For simplicity, the unshifted structure is still used for presenting the network.

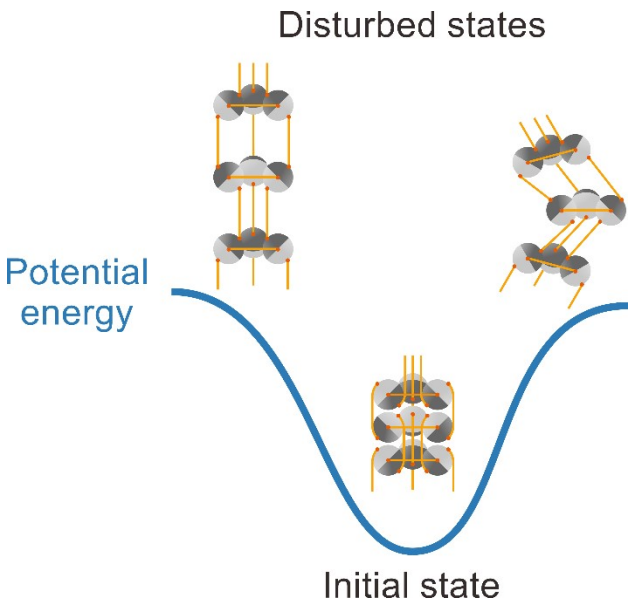

Fig. S8. Schematic illustration of the robustness of the 3D chiral network.

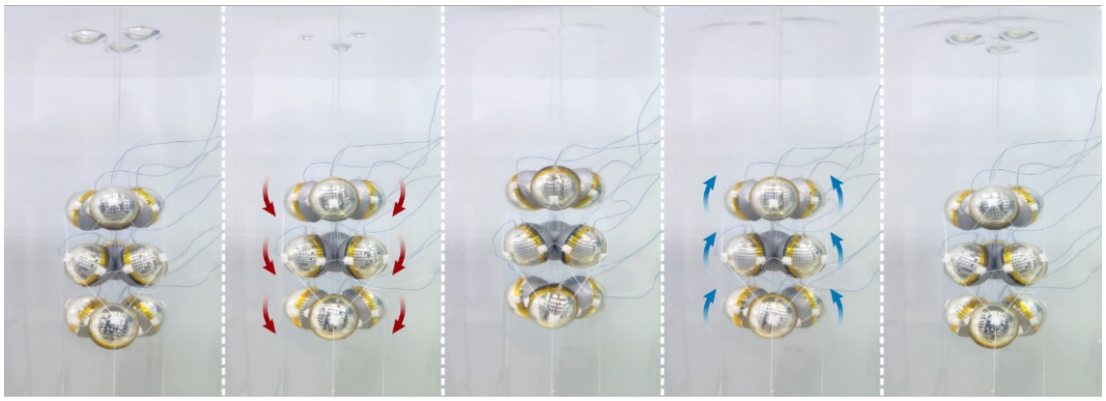

Fig. S9. Motion process of the parallel network under vertically undulating agitations in water.

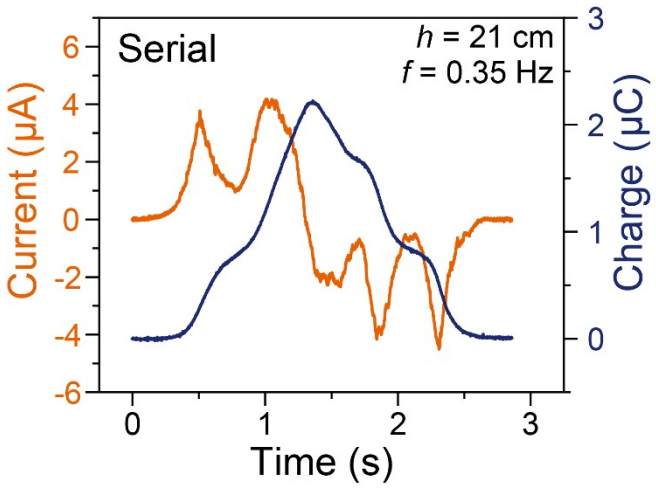

Fig. S10. Short-circuit current and transferred charges of the serial network under a single vertical agitation in water.

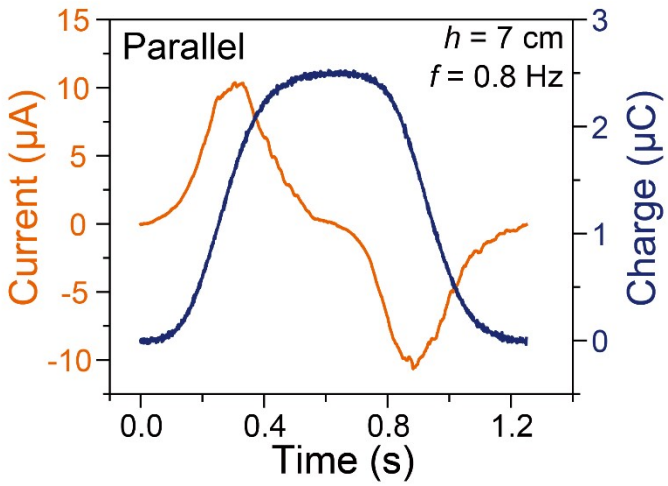

Fig. S11. Short-circuit current and transferred charges of the parallel network under a single vertical agitation in water.

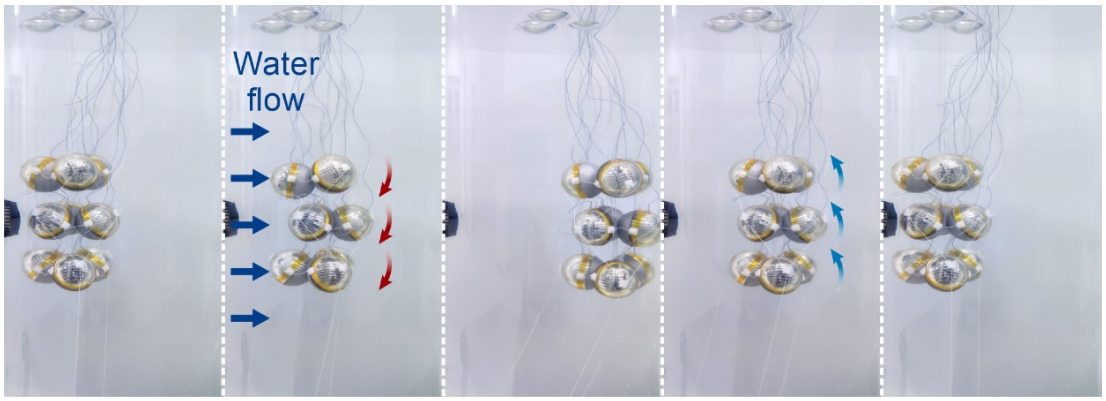

Fig. S12. Motion process of the parallel network under the lateral agitation in water.

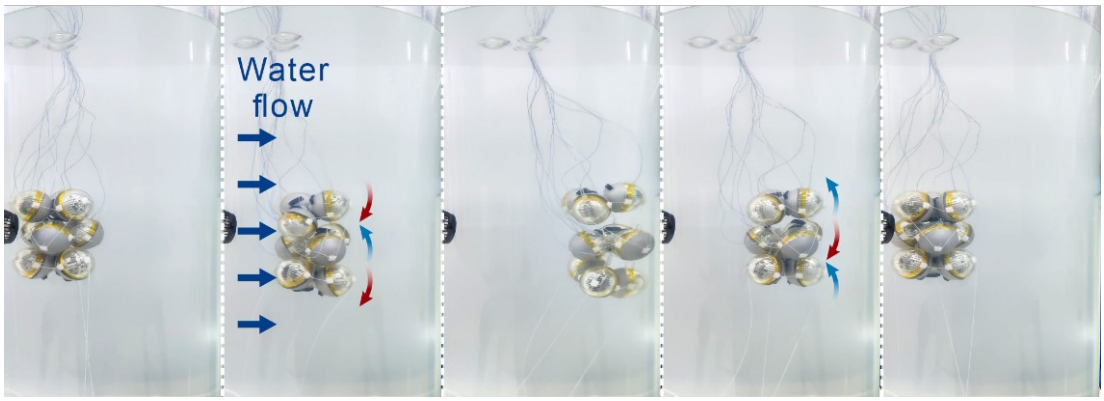

Fig. S13. Motion process of the serial network under the lateral agitation in water.

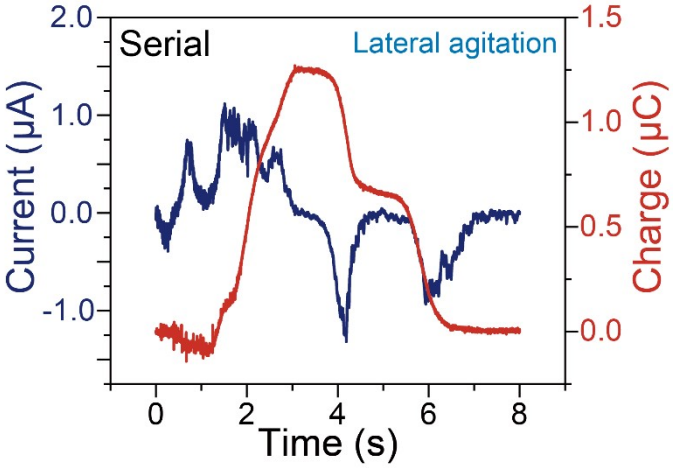

Fig. S14. Short-circuit current and transferred charges of the serial network under a single lateral agitation in water.

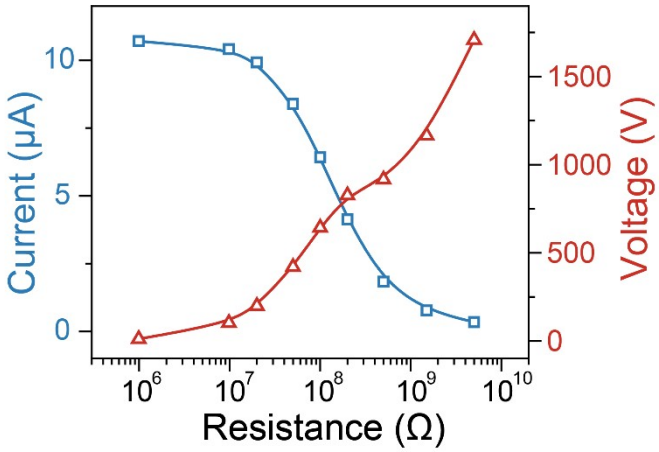

Fig. S15. Peak current and load voltage of the parallel network under agitations with h = 7 cm and f = 0.8 Hz in water.

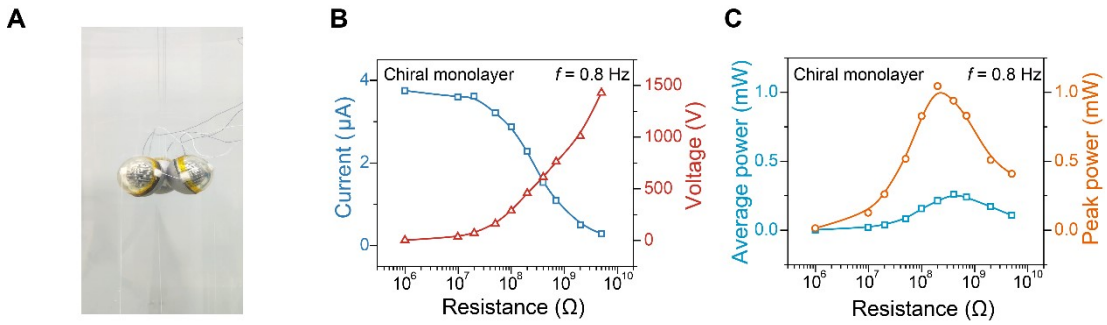

Fig. S16. The monolayer network in water. (A) Photograph of the monolayer network. (B) Peak current and load voltage of the monolayer network. (C) Average power and peak power of the monolayer network with different resistive loads. The agitation frequency is 0.8 Hz.